대 한 체 질 인 류 학 회 지
Korean J Phys Anthropol
21(1): 55 ~ 68, 2008

Chios Gum Mastic Induces Cell Cycle Arrest and Apoptosis in YD9 Human Oral Squamous Carcinoma Cells

Jae-Hyoun Park, Gyoo-Cheon Kim, Hyun-Ho Kwak, In-Ryoung Kim, Seung-Eun Lee, Jin Chung[1], Hae-Ryoun Park[2], Sang-Hun Shin[3], Soo-Hyun Choi[4], Chul-Hoon Kim[4,5], Chang-Ok Nam[4], Bong-Soo Park

Department of Oral Anatomy, [1]Department of Oral Microbiology, [2]Department of Oral Pathology, [3]Department of Oral and Maxillofacial Surgery, School of Dentistry, Pusan National University, [4]Hyowon Dental research [5]Department of Oral and Maxillofacial Surgery, College of Medicine, Dong-A University Medical Center

Abstract : Chios gum mastic (CGM) is obtained from the stem and leaves of *Pistacia lentiscus* trees and has been extensively used for centuries in Mediterranean and Middle Eastern countries, both as a dietary supplement and herbal remedy. This study was undertaken to examine *in vitro* effects of cytotoxicity and growth inhibition, and the molecular mechanism underlying modulation of cell cycle and induction of apoptosis in YD9 human oral squamous carcinoma cell line treated with CGM.

The viability of YD9 cells and human normal keratinocyes (HaCaT cells), and the growth inhibition of YD9 cells were assessed by the MTT assay and clonogenic assay respectively. The hoechst staining and DNA electrophoresis were conducted to observe the YD9 cells undergoing apoptosis. YD9 cells were treated with CGM, and Western blotting, immunocytochemistry, confocal microscopy and FACScan flow cytometry were conducted. Mitochondrial membrane potential change and proteasome activity were measured.

CGM treatment on YD9 cells resulted in a does-dependent inhibition of cell growth and induced apoptotic cell death. And tested YD9 cells showed several lines of apoptotic manifestation. Flow cytometric analysis revealed that CGM resulted in G1 arrest in cell cycle progression which was associated with decrease in the protein expression of cyclin D1, cyclin D3, Cdk2 and Cdk4, and increase in the protein expression of $p21^{WAF1/CIP1}$ and p53.

These results demonstrate that CGM induces G1 the cell cycle arrest via the modulation of cell cycle-related proteins, and apoptosis via mitochondria and caspase pathway in YD9 cells, suggesting that CGM can be considered as a novel therapeutic strategy for human oral squamous cell carcinoma from its strong cell cycle arrest and apoptosis-inducing activity.

Key words : Chios gum mastic (CGM), Apoptosis, Human oral squamous carcinoma cell line, Cell cycle arrest

Introduction

The plant *Pistiacia lentiscus L. var. Chia*. grows particularly and almost exculsively in the South region of Chios Island, Greece, and produces a resin, known as Chios gum mastic (CGM). It is obtained from the stem and leaves *of Pistacia lentiscus* trees and has been extensively used for centuries in Mediterranean and Middle Eastern countries, both as a dietary supplement and herbal remedy (Balan *et al.* 2007, He *et al.* 2007).

*This work was supported by for two years Pusan National University research grant.
Correspodence to : Bong-Soo Park (Department of Oral Anatomy, School of Dentistry, Pusan National University)
E-mail : parkbs@pusan.ac.kr

Apoptosis or programmed cell death, is an essential physiological process that is required for the normal development and maintenance of tissue homeostasis. However, apoptosis is also implicated in a wide range of pathological conditions, including immunological diseases, allergy and cancer (Carson and Ribeiro 1993, Ohta and Yamashita 1999). During apoptosis, cells undergo specific morphological and biochemical changes, including cell shrinkage, chromatin condensation, and internucleosomal cleavage of genomic DNA (Wyllie *et al.* 1980, Williams 1991). Multiple lines of evidence indicate that apoptosis can be triggered by the activation of caspase (Thornberry *et al.* 1997). In addition, mitochondria are known to be central death regulators in response to several apoptotic stimuli (Green and Reed 1998).

Carcinoma of the oral cavity, especially oral squamous cell carcinoma (OSCC), are one of the most leading causes of cancer related death and affect nearly 500,000 patients annually world-wide. And OSCC is one of the most malignancies that remain incurable with current therapies (Shen *et al.* 2007).

Recent studies have been demonstrated that the herbal medicine, which had been being used for treatment of allergic diseases in oriental countries, induced apoptosis and cell growth inhibition in cancer cells (Park *et al.* 2001, Kim *et al.* 2003, Park *et al.* 2005, Yoo *et al.* 2005, Pisano *et al.* 2007). Numerous studies have focused on the targeted induction of apoptosis in order to control the unlimited growth of cells. Moreover, induction of apoptosis in the activated cell may promote therapeutic efficiency in a certain case. Therefore, inducing apoptosis of oral suqamous carcinoma cells could be used therapeutically for oral squamous cell carcinoma patients and understanding the mechanism is important.

To date, reports on apoptotic effects of CGM are few. Especially there is no report about the apoptotic effect of CGM on human oral sqauamous carcinoma cell lines. Therefore this study was undertaken to examine *in vitro* effects of cytotoxicity and growth inhibition in YD9 human oral squamous carcinoma cell line treated with CGM, and the molecular mechanism underlying modulation of cell cycle and induction of apoptosis in CGM-treated YD9 cells.

Materials and Methods

1. Reagents

Chios mastic gum was obtained from mastic korea (Seoul, Korea). The following reagents were obtained commercially: Mouse monoclonal anti-human p53 was from BD biosciences (San Diego, CA, USA); Rabbit polyclonal anti-human cytochrome c, caspase-9 and apoptosis-inducing factor (AIF) antibodies were from Upstate (NY, USA); Mouse monoclonal anti-human $p21^{WAF1/CIP1}$, caspase-3, Bax, Bcl-2, DNA fragmentation factor (DFF45), poly (ADP-ribose) polymerase (PARP), cyclin D1, cyclin D3 Cdk2 and Cdk4 antibodies, and goat polyclonal anti-mouse and FITC-conjugated goat anti-mouse and anti-rabbit IgGs were from Santa Cruz Biotechnology (Santa Cruz, CA, USA); Rabbit polyclonal anti-human DFF40 was from Stressgen (San Diego, USA); Mouse monoclonal anti-human cyclin D3 was from Cell Signaling (Danvers, MA, USA); HRP-conjugated sheep anti-mouse and anti-rabbit IgGs were from Amershan GE Healthcare (Little Chalfont, UK); Suc-LLVY-AMC was from Calbiochem (EMD Biosciences, Germany); 5,5′,6,6′-tetrachloro-1,1′,3,3-tetraethylbenzimidazol carbocyanine iodide (JC-1) was from Molecular Probes (Eugene, OR, USA); Dulbecco's modified Eagle's medium (DMEM) and fetal bovine serum (FBS) were from Gibco (Gaithersburg, MD, USA). Dimethyl sulfoxide (DMSO), Hoechst 33342, RNase A, proteinase K, aprotinin, leupeptin, PMSF, thiazolyl blue tetrazolium bromide, crystal violet and propidium iodide (PI) were from Sigma (St. Louis, MO, USA). SuperSignal West

Pico enhanced chemiluminescence Western blotting detection reagent was from Pierce (Rockford, IL, USA).

2. Cell culture

Human keratinocytes (HaCaT cells) were purchased from the ATCC (Rockville, MD, USA). Human oral squamous carcinoma cells (YD9 cells) kindly provided by Professor Jin Kim (Department of Oral Pathology, College of Dentistry, Yonsei University, Seoul, Korea) and HaCat cells were maintained at 37˚C with 5% CO_2 in air atmosphere in Dulbecco's modified Eagle's medium (DMEM) with 4 mM L-glutamine, 1.5 μg/L sodium bicarbonate, 4.5 g/L glucose and 1.0 mM sodium pyruvate supplemented with 10% fetal bovine serum (FBS).

3. Chios gum mastic (CGM) treatment

Twenty four hours after HaCaT and YD9 cells were subcultured, the original medium was removed. The cells were washed with phosphate-buffered saline (PBS) and then incubated in the same fresh medium. CGM from a stock solution was added to the medium to obtain 5, 10, 25, 50, 100 μg/mL concentrations of the drug. Stock solutions of CGM (100 mg/mL) made by dissolving the drug in DMSO were kept frozen at −20˚C until use. The concentrations of DMSO, 0.002 -0.1% (vol/vol) used in this study, both as a vehicle for CGM and as a control, had no effect on HaCaT and YD9 cells proliferation in our preliminary studies.

4. Determination of viability and proliferation, and morphological assessment of apoptosis

1) MTT assay

Cells were placed in a 96-well plate and incubated for 24 h. Then cells were treated with various concentration of CGM (5, 10, 25, 50, 100 μg/mL) for 24 h and 50 μg/mL CGM for various time points (8, 16, 24, 48, 72 h). And then cells were treated with 500 μg/mL of thiazolyl blue tetrazolium bromide (MTT solution). Cells were incubated at 37˚C with 5% CO_2 for 4 h. And then the medium was aspirated and formed formazan crystals were dissolved in the mixture solution of 75 μL DMSO and 75 μL absolute ethanol. Cell viability was measured by an ELISA reader (Sunrise Remote Control, Tecan, Austria) at 570 nm excitatory emission wavelength. Since viability and proliferation assays demonstrated evident induction of YD9 cell death at 50 μg/mL CGM, this concentration was utilized for further assessment of apoptosis induced by CGM.

2) Hoechst staining for assessing nuclear apoptosis

Cells were observed and photographed under an IMT-2 inverted microscope (Olympus, Japan). Then cells were harvested for 24 h, and the cell suspension was centrifuged onto a clean, fat-free glass slide with a cytocentrifuge. Cells were stained in 4 μg/mL Hoechst 33342 for 30 min at 37˚C and fixed for 10 min in 4% paraformaldehyde. The samples were observed and photographed under an epifluorescence microscope (Carl Zeiss, German). The number of cells that showed condensed or fragmented nuclei was determined by a blinded observer from a random sampling of 250～300 cells per experiment. Three independent experiments were conducted.

3) Clonogenic (colony-forming) assay

YD9 cells were plated into 6-well culture plate (250 cells/well) and allowed to adhere for 8 h before treatment. Culture medium containing CGM ranging from 5 to 25 μg/mL or without CGM was added to cells and incubated for 7 days. After this time, cells were then rinsed with PBS, fixed with 100% methanol and stained with a filtrated solution of 0.5% (w/v) crystal violet for 10 min. The wells were then washed with tap water and dried at room temperature. The colonies, defined as groups of ≥50 cells, were scored manually and photographed under an IMT-2 inverted microscope (Olympus, Japan). Clonogenic survival was

expressed as the percentage of colonies formed in CGM-treated cells with respect to control cells. Three independent experiments were conducted.

5. DNA electrophoresis

2×10^6 cells were resuspended in 1.5 mL of lysis buffer [10 mM Tris (pH 7.5), 10 mM EDTA (pH 8.0), 10 mM NaCl and 0.5% SDS] into which proteinase K (200 μg/mL) was added. After samples were incubated overnight at 48˚C, 200 μL of ice cold 5 M NaCl was added and the supernatant containing fragmented DNA was collected after centrifugation. The DNA was then precipitated overnight at −20˚C in 50% isopropanol and RNase A-treated for 1 h at 37˚C. The DNA from 10^6 cells (15 μL) was equally loaded on each lane of 2% agarose gels in Tris-acetic acid/EDTA buffer containing 0.5 μg/mL ethidium bromide at 50 mA for 1.5 h.

6. Proteasome activity

After treated with 50 μg/mL CGM for various time points, cells were lysed in proteasome buffer [10 mM Tris-HCl, pH 7.5, 1 mM EDTA, 2 mM ATP, 20% glycerol, and 4 mM dithiothreitol (DTT)], sonicated, and then centrifuged at 13,000 g at 4˚C for 10 min. The supernatant (20 μg of protein) were incubated with proteasome activity buffer [0.05 M Tris-HCl, pH 8.0, 0.5 mM EDTA, 50 μM Suc-LLVY-AMC] for 1 h at 37˚C. The intensity of fluorescence of each solution was measured by a modular fluorimetric system (Spex Edison, USA) at 380 nm excitatory and 460 nm emission wavelengths. All readings were standardized using the fluorescence intensity of an equal volume of free AMC solution (50 μM).

7. Western blot analysis

Cells (2×10^6) treated with CGM were washed twice with ice-cold PBS, resuspended in 200 μL ice-cold solubilizing buffer [300 mM NaCl, 50 mM Tris-Cl (pH 7.6), 0.5% Triton X-100, 2 mM PMSF, 2 μL/mL aprotinin and 2 μL/mL leupeptin] and incubated at 4˚C for 30 min. The lysates were centrifuged at 14,000 revolutions per min for 15 min at 4˚C. Protein concentrations of cell lysates were determined with Bradford protein assay (Bio-Rad, Richmond, CA, USA) and equivalent amounts were loaded onto 7.5～15% SDS/PAGE. The gels were transferred to Nitrocellulose membrane (Amersham Pharmacia Biotech, Piscataway, UK) and reacted with each antibody. Immunostaining with antibodies was performed using SuperSignal West Pico enhanced chemiluminescence substrate and detected with Alpha Imager HP (Alpha Innotech, San Leandro, USA). Equivalent protein loading was confirmed by Ponceau S staining.

8. Assessment of mitochondrial event

1) Assay of mitochondrial membrane potential (MMP)

JC-1 was added directly to the cell culture medium (1 μM final concentration) and incubated for 15 min. The medium was then replaced with PBS, and cells were resuspended in 10 μg/mL of methanol and incubated at 37℃ for 30 min. Flow cytometry to measure MMP was performed on a Epics XL (Beckman Coulter, FL, USA). Data were acquired and analyzed using EXPO32 ADC XL 4 color software. The analyzer threshold was adjusted on the FSC channel to exclude noise and most of the subcellular debris.

2) Immunofluorescent staining

Cells were cytocentrifuged and fixed for 10 min in 4% paraformaldehyde, incubated with each primary antibody for 1 h, washed 3 each for 5 min, and then incubated with FITC-conjugated secondary antibody for 1 hr at room temperature. Cells were mounted with PBS. Fluorescent images were observed and analyzed under Zeiss LSM 510 laser-scanning confocal microscope (Göettingen, Germany).

9. Quantification of DNA hypoploidy and cell cycle phases by flow cytometry

Cell cycle progression was determined at multiple time points up to 72 h. At each time point, cells were harvested by trypsinization and ice cold 95% ethanol with 0.5% Tween 20 was added to the cell suspensions to a final concentration of 70% ethanol. Fixed cells were pelleted, and washed in 1% BSA-PBS solution. Cells were resuspended in 1 mL PBS containing 11 Kunitz U/mL RNase, incubated at 4℃ for 30 min, washed once with BSA-PBS, and resuspended in PI solution (50 μg/mL). After cells were incubated at 4℃ for 30 min in the dark, washed with PBS, and filtered through a 20 μm nylon mesh. DNA content were measured on a cytomics FC500 flow cytometry (Beckman Coulter, Fla., USA) and data was analyzed using the Multicycle software which allowed a simultaneous estimation of cell-cycle parameters and apoptosis.

10. Statistical analysis

Three independent experiments were performed for each experimental group and each experiment was performed in triplicate. The results of the experimental and control groups were compared for statistical significance ($p < 0.001$, 0.01 and 0.05) using paired T-test statistical method by SPSS for Win 12.0. for summary data.

Results

1. CGM reduced viability and inhibited the growth in YD9 cells

To investigate whether CGM reduced the viability of YD9 cells and HaCaT cells, MTT assay was conducted. CGM produced a significant time-dependent decrease in the viability of YD9 cells over a period of 72 h. Treatment of YD9 cells with 50 μg/mL CGM prominently induced cell death in a time-dependent manner (Fig. 1A). The viability of YD9 cells treated with CGM 50 μg/mL for 24 h significantly reduced whereas the viability of HaCaT cells treated with CGM 50 μg/mL for 24 h slightly reduced (Fig. 1B). Since the dose required for half-maximal inhibition of viability in YD9 cells was ~CGM 50 μg/mL, this single concentration was utilized for further assessment of apoptosis.

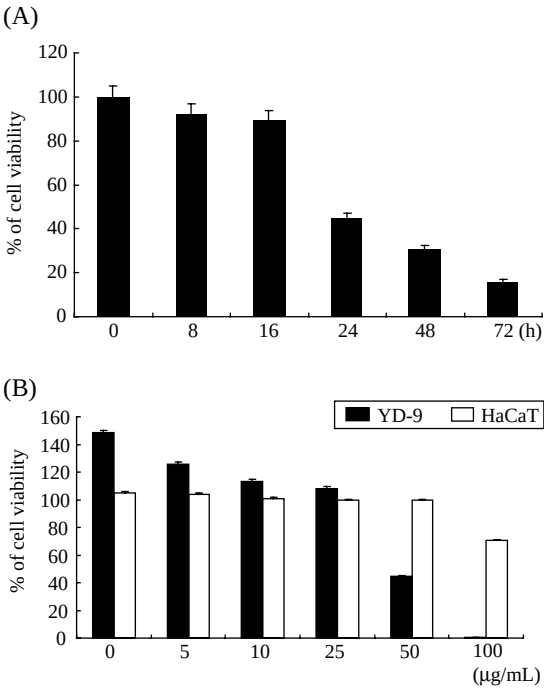

Fig. 1. Effect of CGM treatment on viability of YD9 and HaCat cells as determined by MTT assay. (A) After treatment with 50 μg/mL CGM, viability was undertaken at various time points. CGM at 50 μg/mL reduced viability of YD9 cells in a time-dependent manner (16 h ~ 72 h, $p < 0.001$). Three independent assays were performed. Values are means ± SD of triplicates of each experiment (B) 24 h after CGM treatment (0 ~ 100 μg/mL), the viability of YD9 and HaCaT cells was measured. CGM produced a significant does-dependent decrease in viability of YD9 cells but not HaCaT cells ($p < 0.001$ at 50 μg/mL and 100 μg/mL compared with HaCat cells). Three independent assays were performed. Values are means ± SD of triplicates of each experiment.

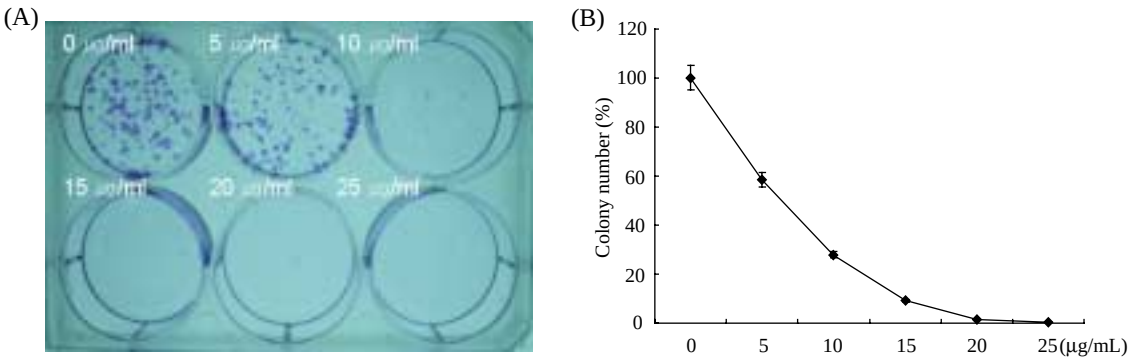

Fig. 2. YD9 cells were cultured in the presence of the indicated concentrations (0～25 μg/mL) of CGM for 7 days. (A) The photograph showing colony formation in YD9 cells. (B) The growth of CGM treated groups is expressed as percentage of control. Note that CGM at low concentrations significantly inhibited the growth of YD9 cells (0～5 μg/mL, $p<0.001$; 5～20 μg/mL, $p<0.01$). Three independent assays were performed. Values are means±SD of triplicates of each experiment.

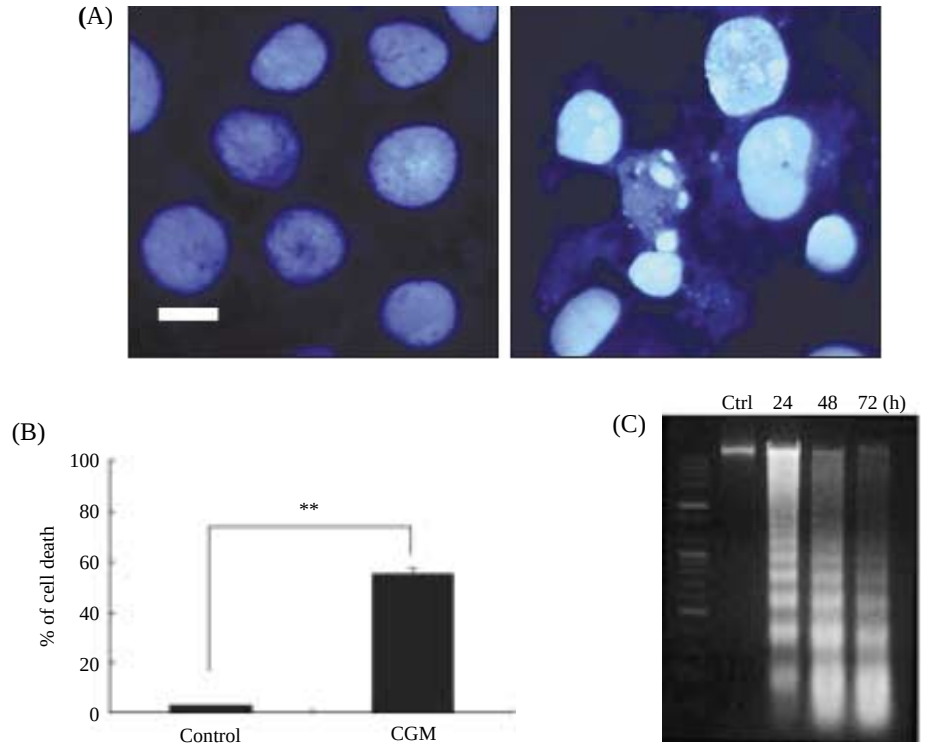

Fig. 3. Demonstration of apoptosis in YD9 cells treated with 50 μg/mL CGM. (A) Immunofluorescent micrographs after Hoechst staining. Control cells showing typical round nuclei (left panel). Cells treated with CGM for 24 h show the production of nuclear condensation or fragmentation (right panel). Scale bar, 10 μm. (B) The values below micrographs are the mean±SD of the means of apoptotic cells as determined by Hoechst staining. The results presented are representatives of three independent experiments. **, $p<0.01$. (C) DNA electrophoresis. The control group (ctrl) which did not have any treatment, showed no DNA fragmentation. Cells treated for 24, 48, 72 h clearly showed DNA degradation characteristic of apoptosis with a ladder pattern of DNA fragments.

To investigate whether CGM inhibited the growth of YD9 cells, clonogenic assay was performed. After exposure to CGM for 7 days, the inhibition of colony formation was determined and was shown in Fig. 2. The CGM dose-dependently inhibited colony formation. The values on colony formation were 100% (control cells), 58.7% (5 μg/mL CGM treated cells), 27.9% (10 μg/mL CGM treated cells), 9.1% (15 μg/mL CGM treated cells), 1.4% (20 μg/mL CGM treated cells) and 0.5% (25 μg/mL CGM treated cells).

2. CGM induced apoptosis in YD9 cells

The incubation of YD9 cells with 50 μg/mL CGM resulted in morphological and biochemical changes associated with apoptosis. Hoechst stain demonstrated that CGM induced a change in nuclear morphology. Compared with the typical round nuclei of the control cells, YD9 cells treated with 50 μg/mL CGM for 24 h displayed condensed and fragmented nuclei (Fig. 3A, B). DNA fragmentation was demonstrated by DNA electrophoresis. YD9 cells treated with CGM at 24 h, 48 h and 72 h showed DNA degradation characteristic of apoptosis, with a ladder pattern of DNA fragments (Fig. 3C). Caspase-9, caspase-3, PARP and DFF45 (ICAD) activation were also demonstrated. The Western blotting study showed that CGM treatment at various time points induced degradations of caspase-9, caspase-3, PARP and DFF45 (ICAD), and produced caspase-9 34 kDd and 17 kDa, caspase-3 17 kDa, PARP 85 kDa, and DFF45 34 kDa and 11 kDa cleaved products (Figs. 4, 5A). And confocal microscopy showed that CGM led to the translocation of DFF40 (CAD) from cytosol onto the nuclei (Fig. 5B).

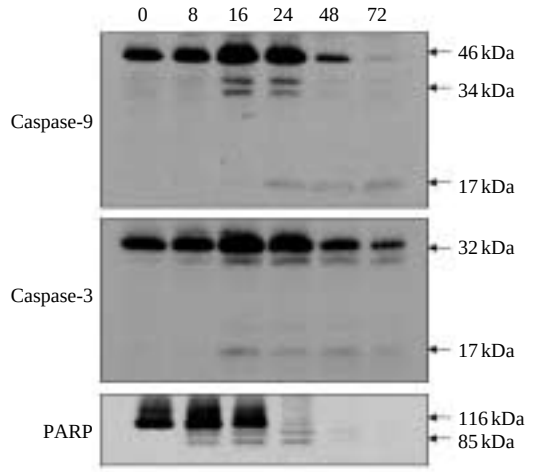

Fig. 4. Western blotting analyses of caspase-9, caspase-3, and PARP. CGM treatment induced caspase-9, caspase-3 and PARP degradation, and produced the processed caspase-9 34 kDa and 17 kDa, caspase-3 17 kDa, and PARP 85 kDa cleaved products.

3. Mitochondrial events were involved in CGM-induced apoptosis of YD9 cells

To dissect the molecular mechanism underlying CGM-inducing apoptosis in YD9 cells, alteration of

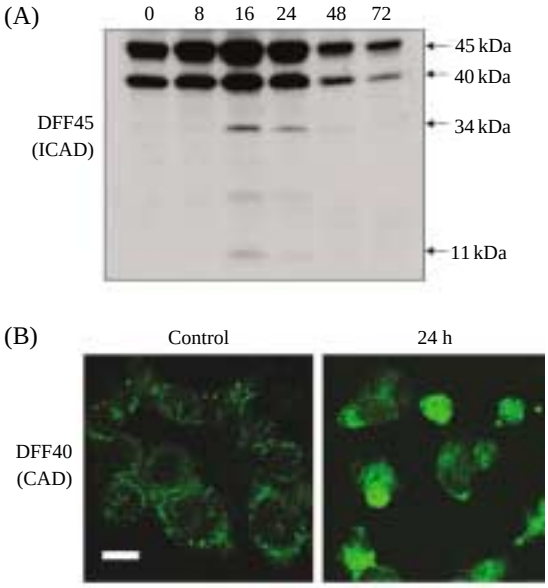

Fig. 5. (A) Western blotting analyses of DFF45 (ICAD). CGM treatment induced DFF45 degradation, and produced the processed DFF45 34 kDa and 11 kDa cleaved products (B) Confocal microscopy showing the translocation of DFF40 (CAD) from cytosol onto the nuclei. Scale bar, 10 μm.

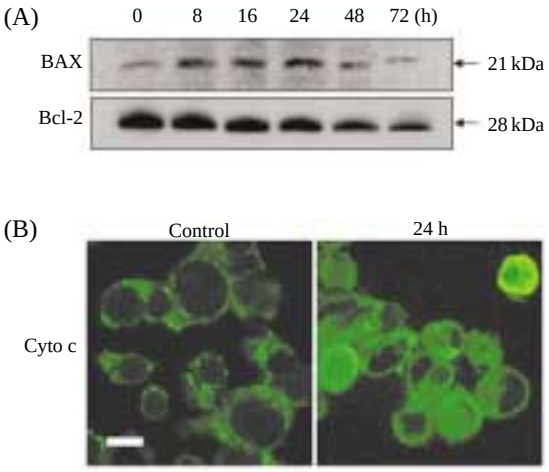

Fig. 6. Bax, Bcl-2, and cytochrome c involve apoptosis in YD9 cells treated with CGM at 50 μg/mL. (A) Western blotting analyses of Bax and Bcl-2. Expression level of Bax significantly increased compared to the control in a time-dependent manner. Compared with Bax expression, expression level of Bcl-2 decreased compared to the control in a time-dependent manner. (B) Confocal microscopy showing the release of cytochrome c from mitochondria into the cytosol. cyto c, cytochrome c. Scale bar, 10 μm.

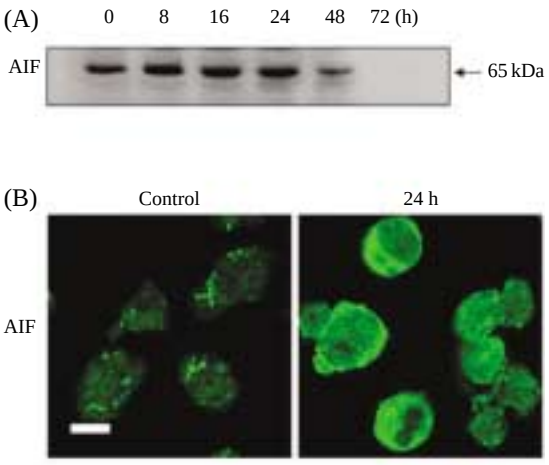

Fig. 7. AIF involves apoptosis in YD9 cells treated CGM at 50 μg/mL. (A) Western blotting analysis of AIF. Expression level of AIF increased compared to the control over a period of 24 h. (B) Confocal microscopy showing that AIF was released from mitochondria, and that translocation onto nuclei was evident in YD9 cells. Scale bar, 10 μm.

the expression level of apoptotic factor, Bax and antiapoptotic factor, Bcl-2 was assayed by Western blotting. Whereas the expression level of Bax increased, Bcl-2 decreased after CGM treatment in a time-dependent manner. This data showed the remarkable change of Bax/Bcl-2 ratio (Fig. 6A). And confocal microscopy showed that CGM led to the release of cytochrome c from mitochondria into the cytosol (Fig. 6B).

Western blot assay and confocal microscopy were conducted to examine whether another mitochondrial apoptotic factor, AIF, is involved or not. Expression level of this protein increased till 24 h after treatment of CGM. AIF was shown to release from mitochondria, and translocation onto nuclei was evident in YD9 cells (Fig. 7).

Loss of mitochondrial membrane potential ($\Delta\Psi$m) is known to be common event in many pathways of apoptosis induction. Also in this study, mitochondrial membrane potential ($\Delta\Psi$m) remarkably decreased after treatment of CGM in a time-dependent manner (Fig. 8).

Proteasome activity assay showed that CGM did not abolish proteasome activity (data not shown).

These data strongly support the hypothesis that the

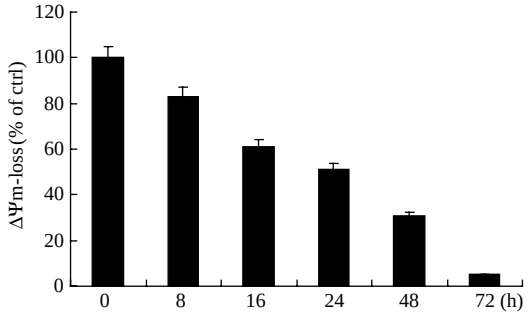

Fig. 8. Mitochondrial membrane potential ($\Delta\Psi$m) at various time points after 50 μg/mL CGM treatment. Mitochondrial membrane potential remarkably decreased in a time-dependent manner (0 h ~ 72 h, $p < 0.001$). Three independent assays were performed. Values are means ± SD of triplicates of each experiment.

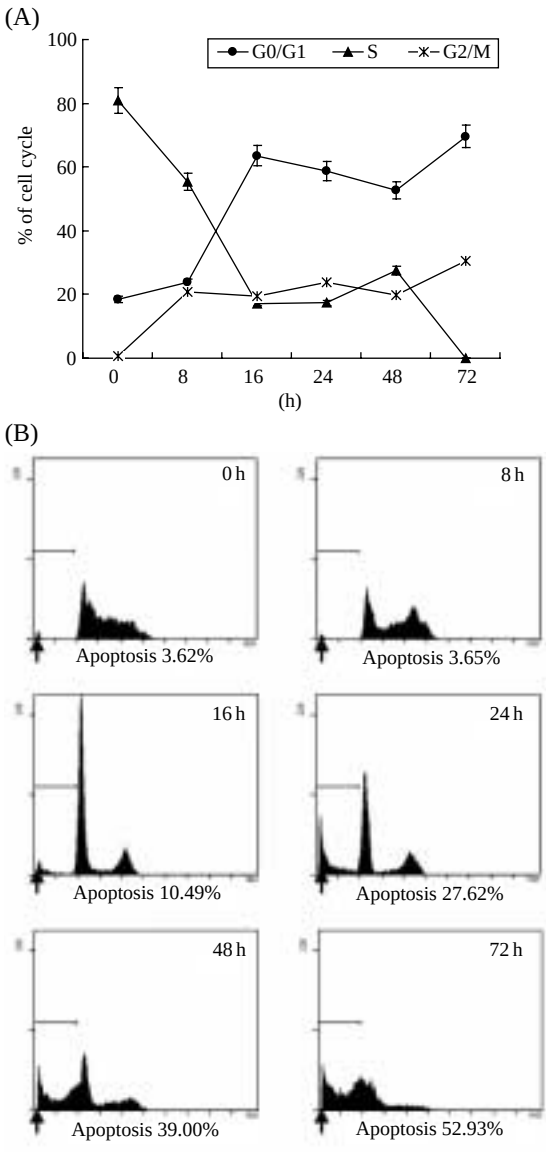

Fig. 9. The kinetic analysis of the effect of 50 μg/mL CGM on YD9 cell cycle progression and induction of apoptosis. These data were analyzed on a FACScan flow cytometry which allows the simultaneous estimation of cell-cycle parameter and apoptosis. (A) The percentages of G0/G1, S and G2/M are depicted. Data shown are representative of three independent experiments. (B) Representative DNA histograms are shown. Time-course analysis of cell cycle distribution after CGM treatment revealed an increase in the percentage of DNA hypoploidy (16 h, $p < 0.01$; 24 h ~ 72 h, $p < 0.001$). Data shown are representative of three independent experiments.

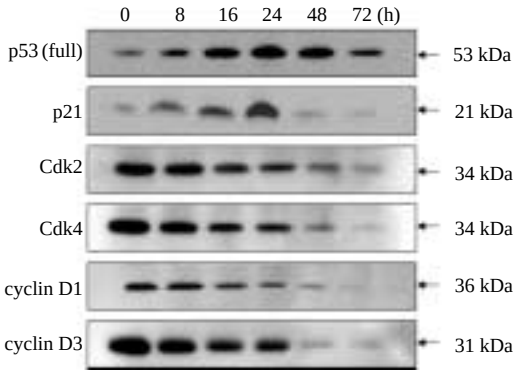

Fig. 10. Western blotting analyses of cell cycle-related proteins. The expression level of Cdk2, Cdk4, cyclin D1 and cyclin D3 decreased time dependently. The expression level of $p21^{WAF1/CIP1}$ and p53 increased time dependently. Note the remarkable increase of $p21^{WAF1/CIP1}$ and p53 at 24 h.

CGM induce apoptosis via mitochondrial pathway in YD9 cells.

4. CGM-inducing apoptosis was related to G1 cell cycle arrest on YD9 cells

Analysis via a flow cytometric method, which allowed the simultaneous estimation of cell cycle parameters and apoptosis, elucidated not only the rate at which CGM altered cell cycle progression but also the correlation between cell cycle progression and cell death (Fig. 9A, B). Time-course analysis of cell-cycle distribution after CGM treatment revealed the increase in the percentage of G0/G1 phase cells, while producing a concomitant fall in the percentage of S phase cells. The increase in the G0/G1 phase cell percentage and concomitant fall in the percentage of S phase cells paralleled an increase in apoptotic cell portions.

To investigate the alternation of cell cycle-related proteins, Westen blotting assay was conducted. Western blotting data showed that expression level of cyclin D1, cyclin D3, Cdk2 and Cdk4 regulating G0/G1 phase decreased in a time-dependent manner. The ex-

pression level of p53 and $p21^{WAF1/CIP1}$ increased in a time-dependent manner ($p21^{WAF1/CIP1}$; till 24 h). Especially at 24 h, the expression level of p53 and $p21^{WAF1/CIP1}$ remarkably increased (Fig. 10).

Discussion

Herbal medicine use is on the rise. The greater acceptance of herbal medicine by healthcare professionals and the public results partly from lively addressing of their pharmacological mechanism. Numerous studies showed that individual herbal medicines had various pharmacological activities, e.g. antiallergic, antipyretic, analgesic, anti-inflammatory and anticancer effects. For exploration of their pharmacological mechanism, the total extracts (Kim *et al.* 1998, Kim *et al.* 1999, Park *et al.* 2001, Na *et al.* 2002, Kim *et al.* 2003) were used. Recently it reported that the herbal medicine, Chios gum mastic (CGM) obtained from the stem and leaves of *Pistacia lentiscus* trees induces cell cycle arrest and apoptosis in prostate cancer cells (Balan *et al.* 2007, He *et al.* 2007). Irrespective of numerous *in vitro* and *in vivo* studies, action mechanism of most herbal medicines remains elusive.

In MTT assay, CGM produced a significant does-dependent decrease in viability of YD9 cells but not human keratinocytes, HaCaT cells. And in clonogenic (colony forming) assay, CGM at low concentrations (5, 10, 15, 20, 25 μg/mL) significantly inhibited the growth of YD9 cells. These data suggest that CGM could have the potential therapeutic possibility as a novel herbal medicine for prevention against human oral squamous cell carcinoma.

Mitochondria play an important role in apoptosis, as the induction of mitochondrial permeability transition plays in the regulation of apoptosis (Kroemer *et al.* 1997, Green and Reed 1998, Susin *et al.* 1999, Orrenius 2004). Permeabilization of the outer mitochondrial membrane (OMM) is modulated by members of the Bcl-2 family of proteins. Antiapoptotic members, such as Bcl-2 and Bcl-xL, inhibit protein release, whereas pro-apoptotic members, such as Bax and Bak, stimulate this release (Orrenius 2004). This study showed a shift in the ratio of Bax to Bcl-2 by CGM. These results indicate that a shift in the ratio of Bax to Bcl-2 may be the molecular mechanisms by which CMG induces apoptosis of YD9 cells. OMM becomes permeable to intermembrane space proteins such as cytochrome c and AIF (apoptosis inducing factor) during apoptosis (Golab *et al.* 2000). Once released, cytochrome c promotes the activation of pro-caspase-9 directly within apoptosome complex (Li *et al.* 1997). Cytochrome c release and disruption of mitochondrial membrane potential (MMP) are known features in apoptosis triggered by proteasome inhibition (Wagenknecht *et al.* 2000, Marshansky *et al.* 2001). On induction of apoptosis, AIF translocates to the nucleus, resulting in chromatin condensation and large-scale DNA fragmentation (Dauglas *et al.* 2000). This study also showed translocation of AIF from mitochondria onto nuclei, the release of cytochrome c from mitochondria into the cytosol, a siginificant reduction of MMP and product of caspase-9 cleavages. Proteasome is a fundamental non-lysosomal tool that cells use to process or degrade a variety of short-lived proteins. Proteolysis mediated by the ubiquitin-proteasome system is known to be implicated in the regulation of apoptosis (Drexler *et al.* 2000). The proteasome pathway works upstream of the mitochondrial alternations and caspase activation (Orlowski 1999). But our data did not show the reduction of proteasome activity in CGM treated YD9 cells (data not shown). Therefore this study has demonstrated that these representive mitochondrial events are involved in CGM-induced apoptosis of YD9 cells. Conclusively, we here report for the first time that CGM induces apoptosis of human oral squamous carcinoma cells through mitochondrial pathway significantly.

A common final event of apoptosis is nuclear con-

densation, which is controlled by caspase, DFF, and PARP. DFF triggers both DNA fragmentation and chromatin condensation during apoptosis (Liu *et al.* 1998). In our study, cleavages of caspase-3, DFF45 (ICAD), and PARP were also shown in CGM-treated YD9 cells. Furthermore our confocal microscopy data demonstrated that CGM led to DFF40 (CAD) from cytosol onto translocation of nuclei in YD9 cells.

There have been many studies on the relationship of cell cycle control mechanisms to apoptosis. Cell death typically occurs in cells arrested in a postmitotic phase of the cell cycle (Ucker *et al.* 1994). We have demonstrated that CGM strongly inhibited YD9 cell growth by G1 cell cycle arrest and apoptosis. Our flow cytometry data indicated that the increases in the G0/G1 phase cell percentage and concomitant fall in the percentage of S phase cells paralleled an increase in apoptotic cell portion. In mammalian cells, D-type cyclins are synthesized during the G1 phase and regulate G1/S transi-tion with their partners, Cdks and Cdk inhibitors regulate cell cycle progression by association with cyclin/Cdk complexes (Choi *et al.* 2005) The G1 cell cycle arrest by trichostatin A is thought to be highly dependent on increased cell cycle kinase inhibitor $p21^{WAF1/CIP1}$ (Roh *et al.* 2004). We tested the expression alterations of cell cycle-related proteins after the treatment of CGM. The results showed that the expression level of cyclin D1, cyclin D3, Cdk2 and Cdk4 regulating G0/ G1 phase decreased in a time-dependent manner whereas the expression level of p53 increased in a time-dependent manner. Furthermore, the expression level of Cdk inhibitor $p21^{WAF1/CIP1}$ showed the significant increase at 24 h. In our study, CGM induced G1 phase arrest in YD9 cells, and we could postulate that G1 phase-arresting mechanism of CGM in YD9 cells may be associated with up-regulation of p53 and $p21^{WAF1/CIP1}$, and down-regulation of cyclin D1, cyclin D3, Cdk2 and Cdk4. This data show that significantly up-regulation of $p21^{WAF1/CIP1}$ and p53 plays a crucial role in CGM-induced G1 cell cycle arrest. Although the up-regulated level of $p21^{WAF1/CIP1}$ and p53 may represent their role in this G1 cell cycle arrest, further investigation is needed.

It is now widely appreciated that agents capable of inducing apoptosis in cancer cells potentially lead to the development of mechanism-based prevention and treatment approaches for cancer. Natural products also contain a variety of chemopreventive compounds that have been shown to prevent the development of malignancies (Rao *et al.* 1995, Lin *et al.* 1997) or to inhibit angiogenesis (Huang *et al.* 1991, Huang *et al.* 1994, Arbiser *et al.* 1998, Cao and Cao 1999, Bai *et al.* 2003). Our data obtained from this study also suggest that CGM may be useful for development for cancer prevention and/or therapy as a novel natural product.

Taken collectively, we demonstrated that CGM strongly inhibits YD9 cells proliferation via the modulation of cell cycle-related proteins and induces apoptosis via mitochondria and caspase pathways in YD9 cells. Our experimental data contribute new insights to the role of CGM and support the view that the clinical effect of CGM may depend on its pharmacological efficacy in regulating human oral squamous carcinoma cells. Furthermore we suggest that CGM can be considered as a novel therapeutic strategy for human oral squamous cell carcinoma from its powerful cell cycle arrest and apoptosis-inducing activity.

References

Arbiser JL, Klauber N, Rohan R, van Leeuwen R, Huang MT, Fisher C, Flynn E, Byers HR : Curcumin is an in vivo inhibitor of angiogenesis. Mol Med 4: 376-383, 1998.

Bai X, Cerimele F, Ushio-Fukai M, Waqas M, Campbell PM, Govindarajan B, Der CJ, Battle T, Frank DA, Ye K, Murad E, Dubiel W, Soff G, Arbiser JL : Honokiol, a small molecular weight natural product, inhibits angiogenesis in vitro and tumor growth in vivo. J Biol Chem 278: 35501-35507, 2003.

Balan KV, Prince J, Han Z, Dimas K, Cladaras M, Wyche JH,

Sitaras NM, Pantazis P : Antiproliferative activity and induction of apoptosis in human colon cancer cells treated in vitro with constituents of a product derived from Pistacia lentiscus L. var. chia. Phytomedicine 14: 263-272, 2007.

Cao Y, Cao R : Angiogenesis inhibited by drinking tea. Nature 398: 381, 1999.

Carson DA, Ribeiro JM : Apoptosis and disease. Lancet 341: 1251-1254, 1993.

Choi HJ, Choi YH, Yee S-B, Im E, Jung JH, Kim ND : Ircinin-1 induces cell cycle arrest and apoptosis in SK-MEL-2 human melanoma cells. Mol Carcinog 44: 162-173, 2005.

Dauglas E, Susin SA, Zamzami N, Ferri KF, Irinopoulou T, Larochette N, Prevost MC, Leber B, Andrews D, Penninger J, Kroemer G : Mitochondrio-nuclear translocation of AIF in apoptosis and necrosis. FASEB J 14: 729-739, 2000.

Drexler HC, Risau W, Konerding MA : Inhibition of proteasome function induces programmed cell death in proliferating endothelial cells. FASEB J 14: 65-77, 2000.

Golab J, Stoklosa T, Czajka A, Dabrowska A, Jakobisiak M, Zagozdzon R, Wojcik C, Marczak M, WilK S : Synergistic antitumor effects of a selective proteasome inhibitor and TNF in mice. Anticancer Res 20: 1717-1721, 2000.

Green DR, Reed JC : Mitochondria and apoptosis. Science 281: 1309-1312, 1998.

He M, Li A, Xu CS, Wang SL, Zhang MJ, Gu H, Yang YQ, Tao HH : Mechanisms of antiprostate cancer by gum mastic: NF-kappaB signal as target. Acta Pharmacol Sin 28: 446-452, 2007.

Huang MT, Lou YR, Ma W, Newmark HL, Reuhl KR, Conney AH : Inhibitory effects of dietary curcumin on forestomach, duodenal, and colon carcinogenesis in mice. Cancer Res 54: 5841-5847, 1994.

Huang MT, Lysz T, Ferraro T, Abidi TF, Laskin JD, Conney AH : Inhibitory effects of curcumin on in vitro lipoxygenase and cyclooxygenase activities in mouse epidermis. Cancer Res 51: 813-819, 1991.

Kim GC, Lee SG, Park BS, Kim JY, Song YS, Kim J M, Yoo KS, Huh GY, Jeong MH, Lim YJ, Kim HM, Yoo YH : *Magnoliae flos* induces apoptosis of RBL-2H3 cells via mitochondria and caspase. Int Arch Allergy Immunol 132: 101-110, 2003.

Kim HM, Lee EH, Hong SH, Song HJ, Shin MK, Kim SH, Shin TY : Effect of Syzygium aromaticum extract on immediate hypersensitivity in rats. J Ethnopharmacol 60: 125-131, 1998.

Kim HM. Yi JM, Lim KS : Magnoliae flos inhibits mast cell-dependent immediate-type allergic reactions. Pharmacol Res 39: 107-111, 1999.

Kroemer G, Zamzami N and Susin SA : Mitochondrial control of apoptosis. Immunol Today 18: 44-51, 1997.

Lin JK, Chen YC, Huang YT, Lin-Shiau SY : Suppression of protein kinase C and nuclear oncogene expression as possible molecular mechanisms of cancer chemoprevention by apigenin and curcumin. J Cell Biochem Suppl 28-29: 39-48, 1997.

Li P, Nijhawan D, Budihardjo I, Srinivascula SM, Ahmad M, Alnemri ES, Wang X : Cytochrome c and dATP-dependent formation of Apaf-1/caspase-9 complex initiates an apoptotic protease cascade. Cell 91: 479-489, 1997.

Liu X, Li P, Widlak P, Zou H, Luo X, Garrard WT, Wang X : The 40-kDa subunit of DNA fragmentation factor induces DNA fragmentation and chromatin condensation during apoptosis. Proc Natl Acad Sci USA 95: 8461-8466, 1998.

Marshansky V, Wang X, Bertrand R, Luo H, Duguid W, Chinnadurai G, Kanaan N, Vu MD, Wu J : Proteasomes modulate balance among proapoptotic and antiapoptotic Bcl-2 family members and compromise functioning of the electron transport chain in leukemic cells. J Immunol 166: 3130-3142, 2001.

Na HJ, Jeong HJ, Bae H, Kim YB, Park ST, Yun YG, Kim HM : Tongkyutang inhibits mast cell-dependent allergic reactions and inflammatory cytokines secretion. Clin Chim Acta 319: 35-41, 2002.

Ohta K, Yamashita N : Apoptosis of eosinophils and lymphocytes in allergic inflammation. J Allergy Clin Immunol 104: 14-21, 1999.

Orlowski RZ : The role of the ubiquitin-proteasome pathway in apoptosis. Cell Death Differ 6: 303-313, 1999.

Orrenius S : Mitochondrial regulation of apoptotic cell death. Toxicol Lett 149: 19-23, 2004.

Park BS, Song YS, Yee SB, Lee BJ, Seo SY, Park YC, Kim JY, Kim HM, Yoo YH : Phospho-ser 15-p53 translocate into mitochondria and interacts with Bcl-2 and Bcl-xL in eugenol-induced apoptosis. Apoptosis 10: 193-200, 2005.

Park HI, Jeong MH, Lim YJ, Park BS, Kim GC, Lee YM, Kim HM, Yoo KS, Yoo YH : Szygium aromaticum (L.) Merr. Et Perry (Myrtaceae) flower bud induces apoptosis of p815 mastocytoma cell line. Life Sci 69: 553-566. 2001.

Pisano M, Pagnam G, Loi M, Mura ME, Tilocca MG, Palmieri G, Fabbri D, Dettori MA, Delogu G, Ponzoni M, Rozzo C : Antiproliferative and pro-apoptotic activity of eugenol-related biphenyls on malignant melanoma cells. Mol Cancer 18: 6-8, 2007.

Rao CV, Rivenson A, Simi B, Zang E, Hamid R, Kelloff GJ, Steele V, Reddy BS : Enhancement of experimental colon carcinogenesis by dietary 6-phenylhexyl isothiocyanate. Cancer Res 55: 4311-4318, 1995.

Roh MS, Kim CW, Park BS, Kim GC, Jeong JH, Kwon HC, Suh DJ, Cho KH, Yee SB, Yoo YH : Mechanism of histone deacetylase inhibitor Trichostatin A induced apoptosis in human osteosarcoma cells. Apoptosis 9: 583-589, 2004.

Shen J, Huang C, Jiang L, Gao F, Wang Z, Zhang Y, Bai J, Zhou H, Chen O : Enhancement of cisplatin induced apoptosis by suberoylanilide hydroxamic acid in human oral squamous cell carcinoma cell lines. Biochem Pharmacol 73: 1901-1909, 2007.

Susin SA, Lorenzo HK, Zamzami N, Marzo I, Snow BE, Brothers GM, Mangion J, Jacotot E, Costantini P, Loeffler M, Larochette N, Goodlett DR, Aebersold R, Siderovski DP, Penninger JM, Kroemer G : Molecular characterization of mitochondrial apoptosis-inducing factor. Nature 397: 441-446, 1999.

Thornberry NA, Rosen A, Nicholson DW : Control of apoptosis by proteases. Adv In Pharmacol 41: 155-177, 1997.

Ucker DS, Hebshi LD, Blomquist JF, Torbett BE : Physiological T-cell death: Susceptibility is modulated by activation, aging, and transformation, but the mechanism is constant. Immunol Rev 142: 273-299, 1994.

Wagenknecht B, Hermission M, Groscurth P, Liston P, Krammer PH, Weller M : Proteasome inhibitor-induced apoptosis of glioma cells involves the processing of multiple caspases and cytochrome c release. J Neurochem 75: 2288-2297. 2000.

Williams GT : Programmed cell death: apoptosis and oncogenesis. Cell 65: 1097-1098, 1991.

Wyllie AH, Kerr JF, Currie AR : Cell death: the significance of apoptosis. Int Rev Cytol 68: 251-306, 1980.

Yoo CB, Han KT, Cho KS, Ha J, Park HJ, Nam JH, Kil UH, Lee KT : Eugenol isolated from the essential oil of Eugenia caryophyllata induces a reactive oxygen species-mediated apoptosis in HL-60 human promyelocytic leukemia cells. Cancer Lett 225: 41-52, 2005.

Korean J Phys Anthropol
20(1): 55 ~ 68, 2008

Chios gum mastic에 의한 사람구강편평상피암종세포 세포주기 정지와 세포자멸사 유도에 대한 연구

박재현, 김규천, 곽현호, 김인령, 이승은, 정 진[1], 박혜련[2], 신상훈[3], 조수현[4], 김철훈[4,5], 남창옥[4], 박봉수

부산대학교 치의학전문대학원 구강해부학교실, [1]구강미생물학교실,
[2]구강병리학교실, [3]구강악안면외과학교실, [4]효원치의학연구회,
[5]동아대학교 의과대학 구강악안면외과학교실

간추림 : 식물인 *Pistiacia lentiscus L. var. Chia.*는 그리이스 키오스 섬의 남부지방에서만 서식하며, Chios gum mastic (CGM)으로 알려져 있는 수지를 만들어 낸다. *Pistacia lentiscus* 나무의 줄기와 잎에서 추출한 천연물질인 CGM은 과거 수세기 동안 지중해와 중동 지역 국가들에서 음식 첨가물과 치료약으로 광범히 하게 사용되어 왔었다. 본 연구는 사람구강편평상피암종세포(YD9 cells)에서 CGM의 세포독성과 성장억제 효과, 그리고 세포주기의 변형과 세포자멸사(apoptosis)에 대한 분자생물학적 기전을 알기 위해서 수행하였다.

YD9 세포와 사람정상각화세포(HaCaT)의 생존률 측정은 MTT법을 시행하였고, YD9 세포의 성장억제를 확인하기 위해서는 clonogenic assay를 사용하였다. 세포자멸사가 유도되는 YD9 세포를 관찰하기 위해서 hoechst 염색법과 DNA 전기영동법을 사용하였다. 그리고 YD9 세포에 CGM을 적용한 후, Western blot 분석, 세포면역화학염색, 공초점레이저주사현미경 검경, FACScan flow cytometry, 사립체막 전위변화, proteasome 활성도 측정 등을 시행하였다.

CGM으로 처리된 YD9 세포는 용량 의존적인 세포 성장억제와 세포자멸사에 의한 세포죽음을 보였고, caspase-9, caspase-3, PARP 그리고 DFF45 (ICAD)의 파괴와 분절의 생성, DNA의 조각남, 핵 응축, 사립체막전위의 감소, Bax와 Bcl-2의 분율의 변화, cytochrome c의 사립체에서의 세포질로의 유리, AIF와 DFF40 (CAD)의 핵으로의 이동과 같은 세포자멸사 증거를 보였다. Flow cytometry 분석에서는 cyclin D1, cyclin D3, Cdk2 그리고 Cdk4의 발현의 감소와 $p21^{WAF1/CIP1}$와 p53의 발현 증가와 관계있는 것으로 보여지는 G1 세포주기 정지를 보였다.

이러한 결과는 CGM이 세포주기 관련 단백질들의 변형을 유도한 G1 세포주기정지와 사립체와 caspase 경로를 통한 세포자멸사를 유도함을 명확하게 증명하고 있다. 이와 같은 강력한 세포주기 정지와 세포자멸사 유도능은 CGM이 사람구강편평세포암종의 새로운 치료전략으로서의 가능성을 높여 준다고 생각한다.

찾아보기 낱말 : chios gum mastic (CGM), 세포자멸사, 사람구강편평상피암종세포, 세포주기정지

교신저자 : 박봉수(부산대학교 치의학전문대학원 구강해부학교실)
전자우편 : parkbs@pusan.ac.kr